BOLETIN DE LA SOCIEDAD ESPAÑOLA DE
Cerámica y Vidrio
www.elsevier.es/bsecv

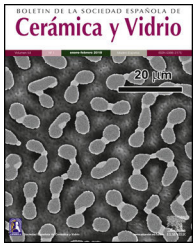

Synthesis and characterization of some calcium aluminate phases from nano-size starting materials

Ahmed A. Amer[a,*], *Hamdy El-Didamony*[a], *Tarek M. El-Sokkary*[b], *Mohamed I. Wahdan*[a]

[a] *Zagazig University, Faculty of Science, Chemistry Department, Zagazig, Egypt*
[b] *Housing and Building National Research Center, Building Materials Chemistry, Cairo, Egypt*

ARTICLE INFO

Article history:
Received 10 March 2020
Accepted 23 July 2020
Available online 14 August 2020

Keywords:
Sol–gel
Calcium aluminate phases
Nano-sized CaO–Al_2O_3 system
Synthesis
Characterization

ABSTRACT

This work aimed to synthesize and characterize some calcium aluminate phases via sol–gel method. These phases were produced by mixing calcium and aluminum nitrates salts [$Ca(NO_3)_2{\cdot}4(H_2O)$ & $Al(NO_3)_3{\cdot}9(H_2O)$] which have been used as starting raw materials to prepare nano-oxides composite of CaO as well as Al_2O_3 in different molar ratio for synthesizing CA, C_2A and C_3A pure phases via Sol–Gel method. The produced powder has been investigated by X-ray Diffraction (XRD), Dynamic Light Scattering (DLS), Fourier-Transform Infrared Spectroscopy (FTIR), Scanning Electron Microscope (SEM) and Thermal Gravimetric as well as Differential Thermal Analyses (TGA & DTA) techniques. The influence of phase composition, calcination temperature as well as the calcination period on the phases' characters was also studied. In addition, the microstructure and the physico-mechanical properties of hydrated phases have been studied. This study concluded that, using nano size starting materials led to the formation of CA and C_3A phases at 1000/1 h and 1200 °C/2 h, respectively which were lower than the traditional methods, while the C_2A phase could not be formed under the normal condition. The crystalline calcium aluminate phases have been formed at earlier calcination temperature with increasing CaO molar ratio.

Síntesis y caracterización de algunas fases de aluminato de calcio a partir de materias primas de tamaño nanométrico

Palabras clave:
Método sol-gel
Fases de aluminato de calcio

RESUMEN

Este trabajo tuvo como objetivo sintetizar por el método sol-gel fases de aluminato de calcio y su caracterización. Se utilizaron como materias primas nitratos de calcio y aluminio [$Ca(NO_3)_2{\cdot}4(H_2O)$ y $Al(NO_3)3{\cdot}9(H_2O)$] para preparar nano-óxidos compuestos de CaO y Al_2O_3

* *Corresponding author.*
E-mail addresses: drahmed.amer@yahoo.com, drahmedamer@zu.edu.eg (A.A. Amer).
https://doi.org/10.1016/j.bsecv.2020.07.006

Sistema CaO-Al_2O_3 de tamaño nanométrico
Síntesis
Caracterización

en diferente relación molar para sintetizar fases puras de CA, C_2A y C_3A. Los polvos sintetizados se caracterizaron por difracción de rayos X, dispersión dinámica de la luz (DLS), espectroscopia infrarroja con transformada de Fourier (FTIR), microscopio electrónico de barrido y análisis térmico diferencial y termogravimétrico (DTA-TGA). Se analizó la influencia de la composición de partida y la temperatura y el periodo de calcinación en las fases sintetizadas y sus características. Además, se estudiaron la microestructura y las propiedades físico-mecánicas de las fases hidratadas. Este estudio concluyó que, el uso de materiales de partida de tamaño nanométrico conduce a la formación de fases CA y C_3A mediante tratamientos a 1.000 y 1.200 °C y que la C_2A no forma en condiciones normales.

Introduction

The binary oxide system CaO–Al_2O_3 has been extensively studied, due to the unique properties developed by the calcium aluminate phases such as rapid strength even at low temperature, high temperature refractory, resistance to wide range of aggressive chemicals, photosensitivity and bioactivity [1]. Therefore, it is used in a wide range of applications like construction industry, ceramics, binders in refractory castable for steel industry, detectors, biomaterials and optical devices [2].

Calcium aluminate cement (CAC) has been made by fusing or sintering together of an appropriate mixture of CaO and Al_2O_3. Limestone (as a source of CaO) and Bauxite (as a source of Al_2O_3) are used as raw materials at high temperature up to 1400 °C. The resultant clinker is finely ground to produce a hydraulic active powder, called CAC [3].

Many investigations about synthesis of calcium aluminates phases have been carried out by using nitrate salts of calcium and aluminum as raw materials [1]. The single phase of calcium aluminate (CA, C_3A & $C_{12}A_7$) has been successfully prepared though adjusting calcium/aluminum molar ratio in the raw materials [1,4]. The CA (CaO–Al_2O_3) phase diagram in ambient air that contains moisture is reported by Chatterjee et al. [5], whereas, that phase diagram in a moisture free atmosphere was determined by Nurse et al. [6]. The diagram includes different phases such as, CA_6, CA_2, CA, $C_{12}A_{14}$ and C_3A, where C = CaO and A = Al_2O_3. Monocalcium aluminate (CA) and dodecacalcium hepta-aluminate ($12CaO{\cdot}7Al_2O_3$, $Ca_{12}Al_{14}O_{33}$ or $C_{12}A_7$ – Mayenite) are common hydraulic active constituents of Calcium Aluminate Cement (CAC), Mayenite phase play an intermediate in the manufacture of Portland cement. Tricalcium aluminate (C_3A – Celite) is a common component of Portland cement (PC), as it plays an important role in the cement setting process, especially in the first stages of hydration process [7].

Many reactions are possible among the calcium and aluminum oxides that lead to different calcium aluminate phases, Singh et al. [8] suggested few reactions for prepared C_3A

$$CA_{(S)} + 2CaO_{(S)} \rightarrow C_3A_{(S)} \quad (1)$$

$$CA_{2(S)} + 5CaO_{(S)} \rightarrow 2C_3A_{(S)} \quad (2)$$

$$C_{12}A_{7(S)} + 9CaO_{(S)} \rightarrow 7C_3A_{(S)} \quad (3)$$

$$C_{12}A_{7(S)} + CA_{(S)} + 11CaO_{(S)} \rightarrow 8C_3A_{(S)} \quad (4)$$

Conventionally, calcium aluminates are produced by solid state sintering reactions. However, this method requires high temperature and produces undesired phases like unreacted lime, alumina and intermediate ($C_{12}A_7$) mayenite in the end product [8]. Combustion synthesis method is also used for preparation calcium aluminates. This technique ensures high purity of products, low processing cost, time as well as energy efficiency and no high temperature furnace process [9]. Mechano-chemical treatment and high energetic attrition milling techniques have been used for calcium aluminates synthesis [10,11].

Pechini and sol–gel methods [12,13] were applied for preparation of calcium aluminates. The sol–gel method is complicated and expensive but produces bulk metal oxides as ceramic, fibbers, films and glasses with enhanced properties like high surface area, high purity, controllable chemical composition as well as nano size particles. Nanoparticles are important for producing nanocomposite or nano size powder. Both of nano γ-alumina and α-alumina are thermally stable at high temperature; however, they are difficult to synthesis. Heat can induce particles growth of powder and will be inconvenient to prepare nanoparticles. The main processes for preparing nano-alumina powder can be either chemical or physical. The physical methods include mechanical milling, flam spray and laser ablation. Whereas, chemical methods involve vapor phases reaction, hydrothermal, co-precipitation, combustion, and sol–gel methods [14].

Nano-CaO can be produced by several methods such as sonochemical [15], precipitation [16], thermal decomposition [17] and sol–gel [18]. The properties of CaO nanoparticles depend on their morphology and its size which affects by high temperature.

The reaction between calcium aluminate phases and free water is called hydration process. It is exothermic and leading to precipitation a mixture of hydrate phases, such as: CAH_{10}, C_2AH_8, C_3AH_6 as well as $Al(OH)_3$ gel. These hydrates are responsible for hardness development and strength, especially monocalcium aluminate (CA), monocalcium dialuminate (CA_2), and dodeca-calcium hepta-aluminate ($C_{12}A_7$) phases. The hydration of CA is responsible for early strength development and that of CA_2 contributes when the main reaction of CAC hydration has already exceeded.

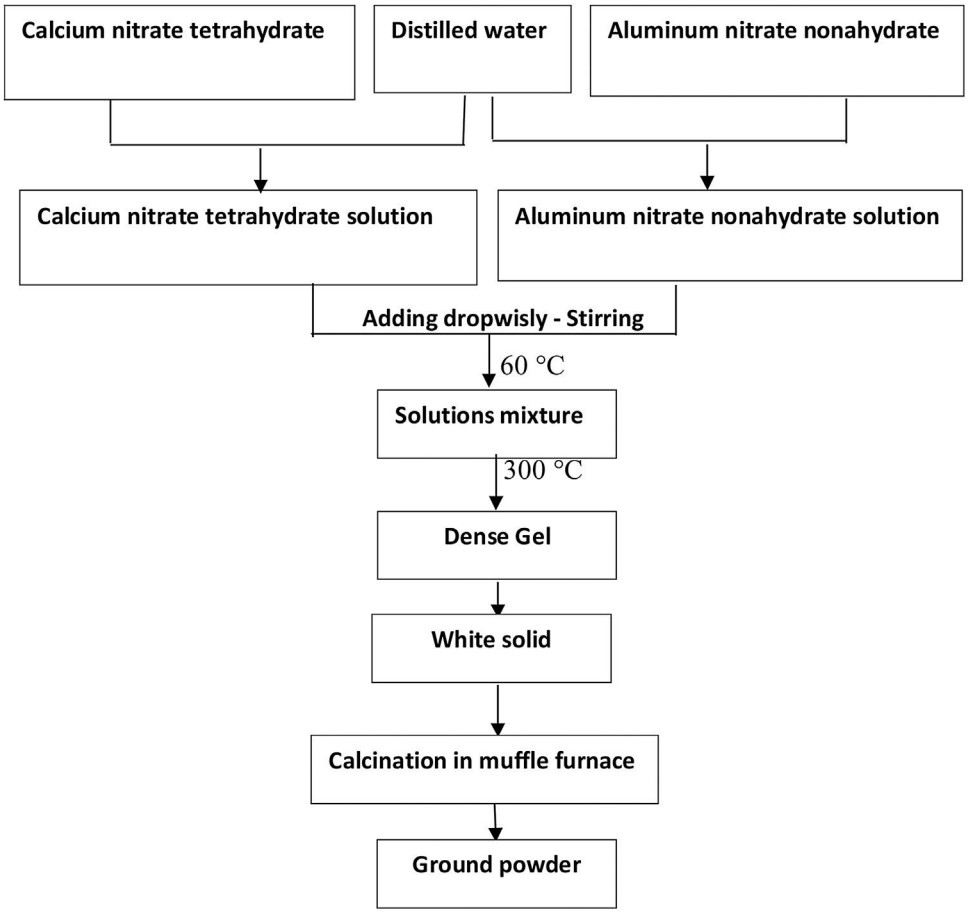

Fig. 1 – Flow chart for preparation calcium aluminate phases powder via sol–gel method.

Hydration of CAC occurs rapidly within the first 24 h, in contrast the hydration of Portland cement (PC); where in Portland cement the hydration reactions occur during 28 days depending on the type of PC, and the reactions can last happening even behind 28 days but in a slower manner [19].

The present work aims to synthesis and characterized of some calcium aluminate phases (CA, C_2A and C_3A) via sol–gel method. The influence of phase composition, calcination temperature as well as the calcination period on the phases' characters was also studied. In addition, the microstructure and the physico-mechanical properties of some hydrated phases have been studied.

Experimental

Raw materials

Calcium nitrate tetrahydrates [$Ca(NO_3)_2{\cdot}4H_2O$] (Mol. Wt., 236.15) and aluminum nitrate nonahydrates [$Al(NO_3)_3{\cdot}9H_2O$] (Mol. Wt., 375.134) are extra pure 98% and produced from Loba Chemie – India, these chemicals have been used as raw materials for synthesis of CA, C_2A and C_3A with appropriate molar ratio (1:2, 2:2 & 3:2) respectively.

Preparation of gel

For the preparation of gel, the stoichiometric requirement of the solution is prepared. The nitrate salts of calcium and aluminum [$Ca(NO_3)_2{\cdot}4(H_2O)$ & $AlNO_3)_3{\cdot}9(H_2O)$] were dissolved in distilled water for preparing CA, C_2A as well as C_3A with appropriate molar ratio. Calcium nitrate solution was dropwisely added to the aluminum nitrate solution with continuous stirring. The liquid "sol" was heated up to 300 °C to remove the nitrates as well as gases. - Water evaporated and solution becomes dense, then fumes of nitrogen oxides were detected. With continuous heating process, a white solid "gel" phase has been formed with disappearing of fumes at the end of the heating process. This method is called aqueous sol–gel method. Scheme of the synthesis is shown in Fig. 1.

Calcination process

The sample was prepared and annealed at different temperatures. The calcination process was done by muffle furnace at different temperatures ranged between 500 and 1200 °C for 1 h. In addition, the phases (CA & C_3A) are calcined at 1000 and 1200 °C, respectively with soaking time 2 as well as 4 h.

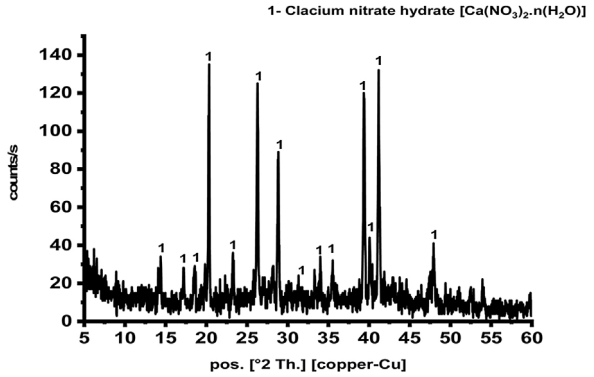

Fig. 2 – XRD pattern of starting material composite preheated at 300 °C.

Preparation of calcium aluminate pastes

Calcium aluminate phases' pastes has been prepared by mixing calcined phases of CA as well as C_3A at 1000 and 1200 °C for 1 & 2 h, respectively with required water of consistency according to ASTM C-191 [20]. Then, each paste has been casted in a cubic steel mold with dimension 2 × 2 × 2 cm. The mold was manually vibrated for few minutes to remove any air bubbles and gave a better compaction paste. Immediately after casting, the mold was kept in a humidity chamber at 100% relative humidity and constant temperature (20 ± 2 °C) for the first 24 h. Hardened cubes were demolded and then cured in 100% humidity for 28 days. After the desired curing time (28 days), the hydration process of the hardened (thee) cubes was stopped though dried in oven at 105 °C for 24 h.

Investigations and techniques

The formed starting oxide composite and the phases have been studied by XRD (Bruker D8 Advance, Cu target, wavelength 1.5 Å, 40 kV, 40 mA), SEM (FEI Quanta 250 FEG-SEM), TGA & DTA (Shimadzu thermogravimetric analyzer TGA-50H, 20 °C/min heating rate), FTIR (JASCO FTIR spectroscope model FT/IR-6100 type A) and DLS (Zetasizer ver. 6.32, and used acetone as a solvent). The hydrated hardened cubes have been examined (compressive strength, porosity as well as bulk density) were determined as described elsewhere [21] and SEM technique.

Results and discussion

Characterization of prepared calcium aluminate phases

The sol–gel method is a good technique for synthesis of advanced materials. It is used at relatively low temperature as compared with the traditional methods. Fig. 2 represents XRD pattern of starting material composite prepared via sol–gel technique which was dried and preheated at 300 °C. It shows only existence calcium nitrate hydrate [$Ca(NO_3)_3{\cdot}n(H_2O)$] in crystalline state, and there is no existence any sign of aluminum nitrate nonahydrate. Aluminum nitrate nonahydrate has been decomposed by heating up to 300 °C and amorphous

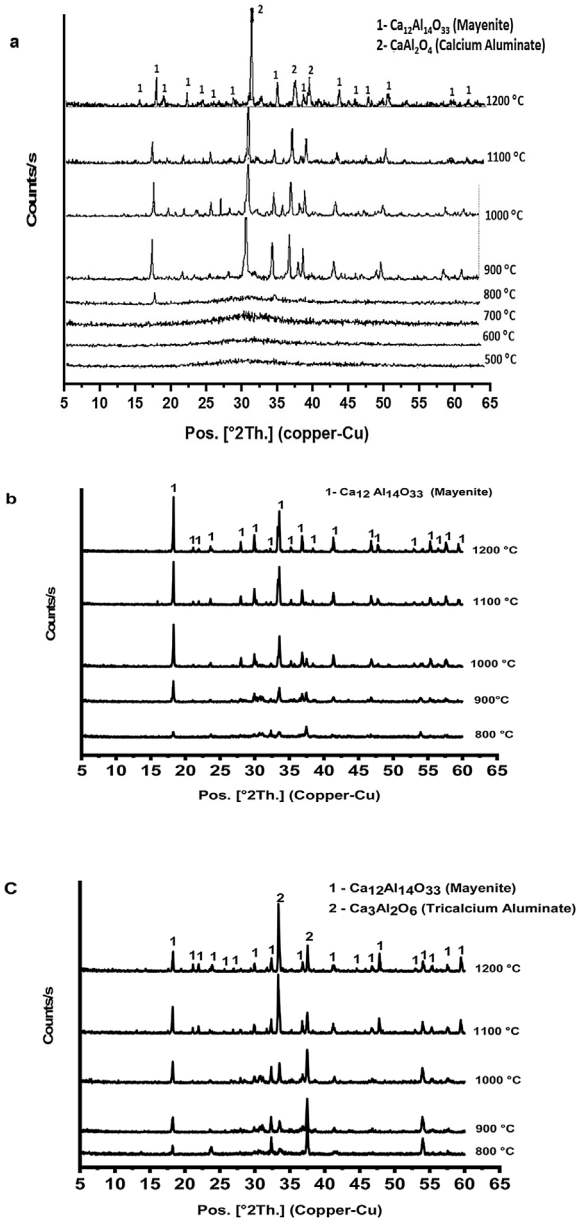

Fig. 3 – XRD pattern of prepared calcium aluminate phases: (a) CA, (b) C_2A and (c) C_3A calcined at different temperatures.

γ-Al_2O_3 was produced according to the following equation

$$2Al(NO_3)_3{\cdot}9H_2O + \Delta(130\text{–}500\,^{\circ}C) \rightarrow Al_2O_3 + 18H_2O + N_2O + 2NO_2 + 2NO + 4O_2$$

At the beginning, H_2O as well as HNO_3 are released in large quantities with increasing heat temperature up to 150 °C. As the reaction continues, a big amount of NO_2 and NO gases are evolved up to 255 °C and at the end, some of N_2O is produced [22] is in agreement with the present result.

Fig. 3 shows XRD patterns (a–c) of prepared calcium aluminate phases (CA, C_2A and C_3A, respectively) at different

temperatures ranged between 500 and 1200 °C for 1 h. It appears that no peaks are formed at 500 up to 700 °C, this means that all constituents become amorphous. Also, amorphous γ-Al_2O_3 did not transform and calcium nitrate hydrate has been decomposed.

$$4Ca(NO_3)_2{\cdot}4H_2O \rightarrow 4CaO + N_2O + 2NO_2 + 4NO + 16H_2O + 4O_2, \quad \Delta H = 369\ kJ/mol$$

Calcium nitrate tetrahydrate loses partially its crystalline water at 120 °C and becomes hydrated with less water molecules which losses all the water molecule subsequently at 155, 160 and 210 °C, then the anhydrous decomposes starting at 561 °C to produce calcium oxide and nitrogen oxide [23,24]. XRD curves in Fig. 3(a–c) exhibits appearance of some peaks at 800 °C, where the amorphous γ-Al_2O_3 transforms to crystalline δ-Al_2O_3 at 750 °C and therefore, crystalline calcium aluminate phases are formed [25]. CA and C_3A phases have been formed starting at 900 °C as shown in Fig. 3(a & c) and mayenite ($Ca_{12}Al_{14}O_{33}$) was also produced. While, mayenite was formed and C_2A did not produced as shown in Fig. 2(b). So, C_2A has been prepared under specific condition at 1250 °C and 25 000 bars [26].

From Fig. 3(a & c) we noticed also that, with increasing calcination temperature from 900 to 1200 °C, the transformation process of CA and C_3A phases to CA phase at 1000 °C. Fig. 3(a) looks better than at 900 °C. However, there is no significant change at 1100 and 1200 °C. In contrast, the transformation to C_3A as in Fig. 3(c) looks better at 1200 °C. Also, with increasing the amount of calcium oxide percent in the constituents as in CA, C_2A and C_3A phases, we can detect a small peak at 800 °C (Fig. 3a–c). Increasing CaO content accelerates the formation of phases at lower temperature.

Fig. 4(a & b) represents the XRD patterns for CA as well as C_3A calcined at 1000 and 1200 °C, respectively for 1, 2 and 4 h. In Fig. 4(a), CA phase pattern showed no significant effect of calcination time on the phase. While, C_3A phase has been affected by the calcination time, therefore the transformation at 2 h is better than 1 h and there is no change at 4 h.

Fig. 5 represents thermal gravimetric and differential thermal analyses (TG and DTA) curves of the starting materials composite preheated at 300 °C. TG and DTA curves exhibit thee endothermic peaks located at 134.8, 422.9 and 585.25 °C. The mass loss of the first step is attributable to the loss of interlayer water below 200 °C (73–200 °C). The weight loss at the second step (300–450 °C) is due to the decomposition of aluminum nitrate hydrate forming Al_2O_3 as well as N_2O. The gas produced from the decomposition of the anhydrous aluminum nitrate has been lost at 300–450 °C. Finally at the last step, the loss weight is attributed to decomposition of anhydrous calcium nitrate at 500–600 °C producing CaO and NO_2.

Fig. 6(a & b) shows the dynamic light scattering (DLS) curves of size distribution for CA and C_3A phases' constituents, respectively at 300, 900, 1000 and 1100 °C. As shown in Fig. 6(a), the CA's particles size at 300 °C is about 93 nm, increased up to 168 nm at 900 °C, then the particles size reduced to 49 nm at 1000 °C and finally increased to 467 nm at 1100 °C. Increasing of size at 900 °C can be explained as a result of the formation of a mixture of monoclinic CA and cubic $C_{12}A_7$ (mayenite) which is bigger in crystal size than CA [27], Increasing the temperature up to 1000 °C induces the transformation of mayenite to CA which is smaller crystal size. CA's particle size increases with increasing the calcination temperature up to 1100 °C.

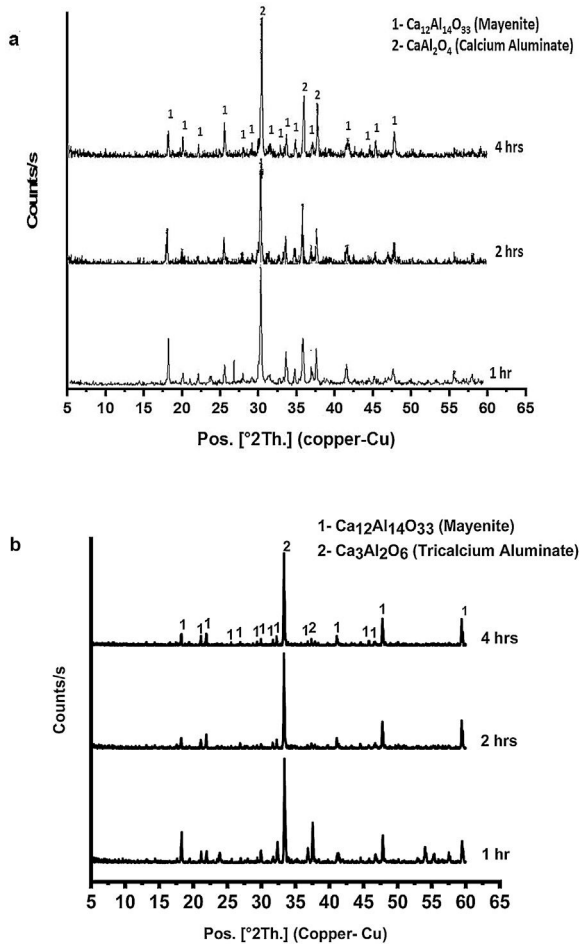

Fig. 4 – XRD pattern of (a) CA and (b) C_3A calcined at 1000 °C and 1200 °C, respectively for different periods.

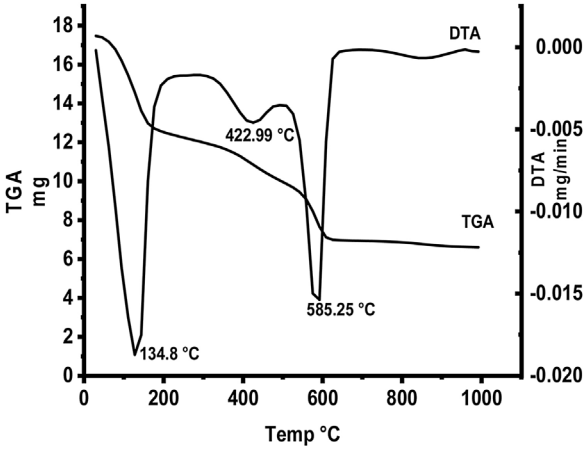

Fig. 5 – TGA and DTA curves of starting materials composite preheated at 300 °C.

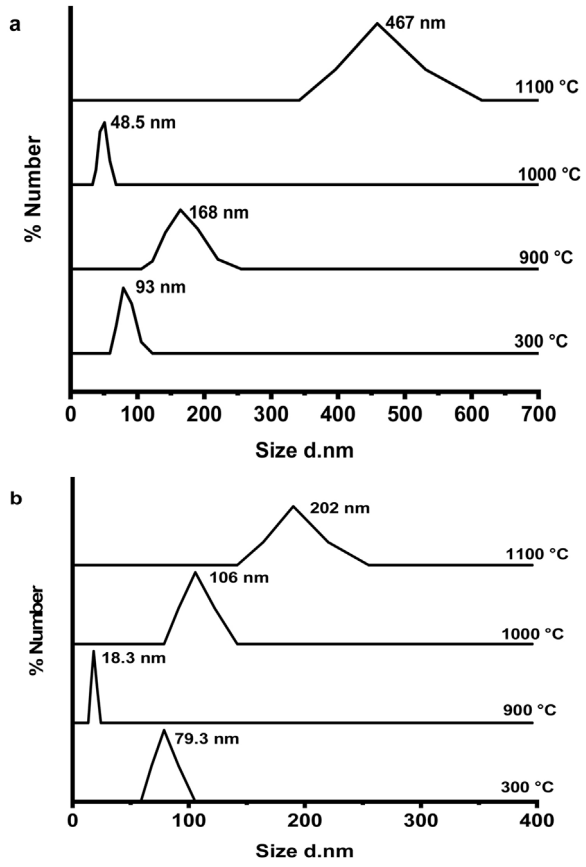

Fig. 6 – DLS curves of size distribution of prepared calcium aluminate phases: (a) CA and (b) C_3A at different temperatures.

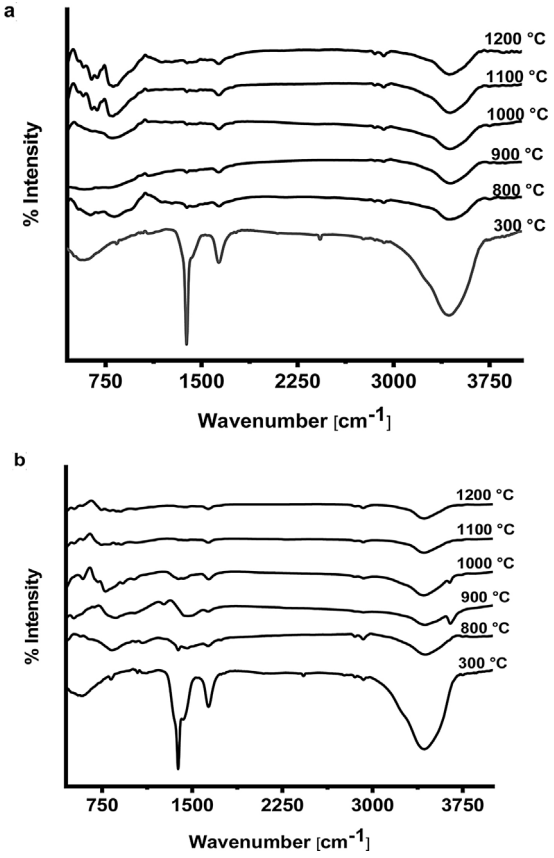

Fig. 7 – FTIR spectra for prepared calcium aluminate phases: (a) CA and (b) C_3A at different temperatures.

Fig. 6(b) represents the C_3A constituent's particle size behavior with increasing the calcination temperature. The particle size of the components at 900 °C is more reduced than the size at 300 °C due to the formation of only cubic mayenite phase with smaller size. Increasing calcination temperature up to 1000 °C as well as 1100 °C, led to an increase in the particle size. This is due to the transformation process of cubic maynite to cubic C_3A, which is bigger crystal size [27].

The FTIR spectra of prepared CA and C_3A phases at different temperatures are shown in Fig. 7(a & b). It is found that, the spectra at 300 °C shows the formation of a characteristic peaks of water at 3400 cm^{-1} as well as at 1700–1600 cm^{-1} due to O–H bending vibration and stretching, this peak become smaller with increasing the calcination temperature up to 1200 °C. The presence of O–H group is due to the existence of absorbed water on the active phase surface. At 1400–1300 cm^{-1} there was a peak due to N–O of nitrate (NO_3^-) which disappeared with increasing temperature starting from 800 up to1200 °C as a sign to complete decomposition. The peak at 2425 cm^{-1} due to atmospheric carbon dioxide (CO_2) appeared at 300 °C then disappeared in the spectra starting from 800 up to1200 °C. A broad peak appeared in all spectra at 1083–300 cm^{-1} is assigned to Al–O due to formation and vibration of tetrahedron AlO_4 and octahedron AlO_6.

Fig. 8 shows the SEM image of starting material composite of the calcium aluminate which preheated at 300 °C for 1 h.

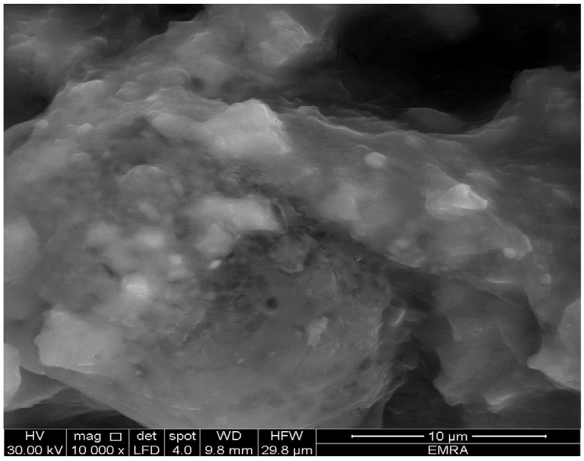

Fig. 8 – SEM image for starting material composite preheated at 300 °C for 1 h.

We can observe non-isolated aggregates particles. It seems like gelatinous or hydrated matter, so there is no existence of porous and it is difficult to measure the particle size.

The image of Fig. 9(a), shows a small extend of adsorbed water and the grain size was found to increase with increasing calcination period (soaking time) (Fig. 9a–c). The grain size of calcined powder at 1000 °C for 1 h has been detected in the range of 36–96 nm, while it becomes around 190–360 nm after

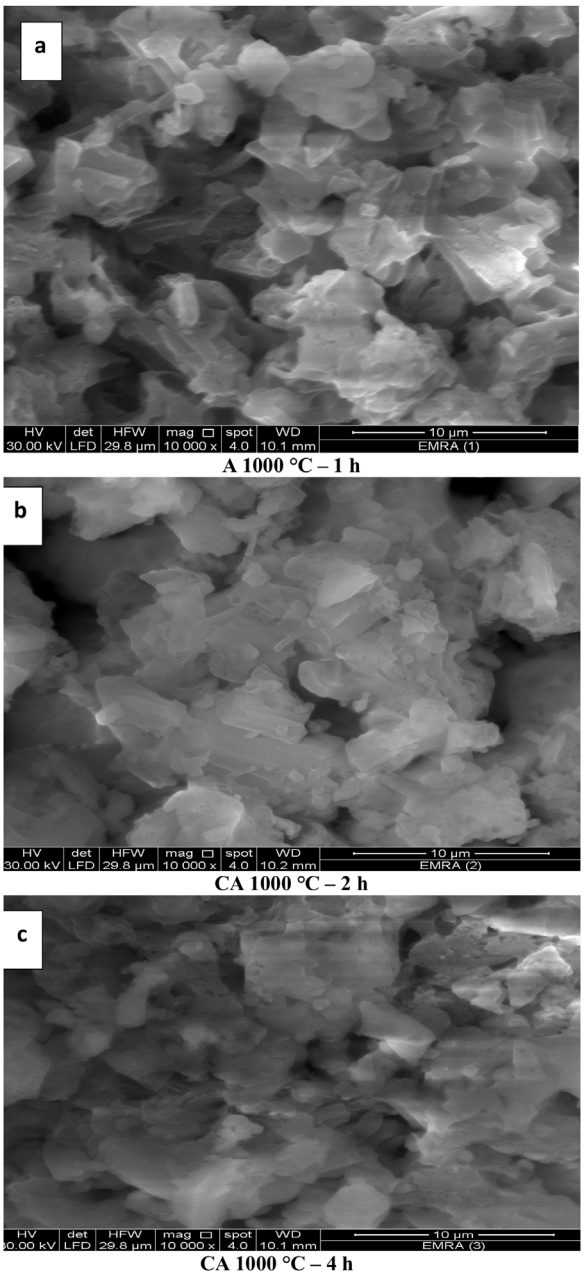

Fig. 9 – SEM images for CA phase calcined at 1000 °C for 1, 2 and 4 h in (a, b and c) images respectively and CA phase calcined at 1100 °C for 1 h in (d) image.

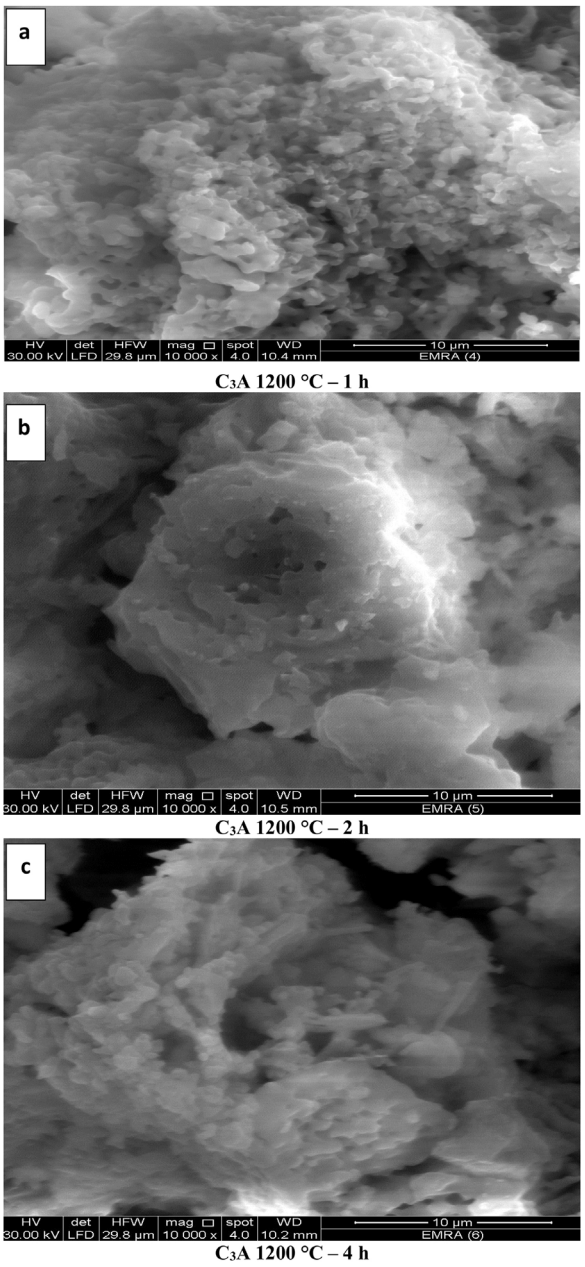

Fig. 10 – SEM images for C_3A phase calcined at 1200 °C for 1, 2 and 4 h in (a, b and c) images in respectively and C_3A phase calcined at 1100 °C for 1 h in (d) image.

2 h. However, the size of calcined powder after 4 h could not be measured because the particles were in coagulated state. The SEM results are in agreement with XRD and DLS analyses. In addition, the grain size has been increased with elevation the calcination temperature followed by decreasing the porosity as in Fig. 9(a & d).

The images of Fig. 10, exhibited an increase in the grain size with increasing the calcination period (soaking time) as in images (a–c). The grain size of calcined powder at 1200 °C for 1 h has been measured in the range of 219–269 nm, but increased up to 348–563 nm for 2 h. Finally, the grain size was found to be in the range of 380–600 nm at period of 4 h. The elevation in the calcination temperature led to an increase in the particle size and decrease in the porosity as shown in Figs. 10(a & d).

Microstructure and physico-mechanical properties of hydrated phases

Fig. 11(a) shows the SEM image of the hydrated CA phase calcined at 1000 °C for 1 h cured in 100% humidity up to 28 days. It is clear that, the presence of composite of monoclinic gibbsite AH_3 and cubic hydrated tricalcium aluminate C_3AH_6 crystals. This is due to the conversion of metastable hexagonal hydrated calcium aluminate CAH_{10} and hydration products of

Table 1 – Mechanical and physical properties of calcined CA and C_3A at (1000/1 h & 1200 °C/2 h) after hydrated for 28 days.

Properties	CA			C_3A		
	Mean	St. Deviation	Variance	Mean	[a]St. Deviation	[b]Variance
Bulk density (g/cm^3)	1.4067	1.53×10^{-2}	2.335×10^{-4}	1.393	1.26×10^{-2}	1.58×10^{-4}
Total porosity (%)	40.017	1.96×10^{-1}	3.82×10^{-2}	12.03	1.86×10^{-1}	3.465×10^{-2}
Comp. strength (MPa)	3.906	2.26×10^{-2}	5.11×10^{-4}	4.983	9.61×10^{-2}	9.23×10^{-3}

[a] St. Deviation (S) $= \sqrt{\sum (X_i - \ddot{X}^2)/(n-1)}$.
[b] Variance $= S^2$.

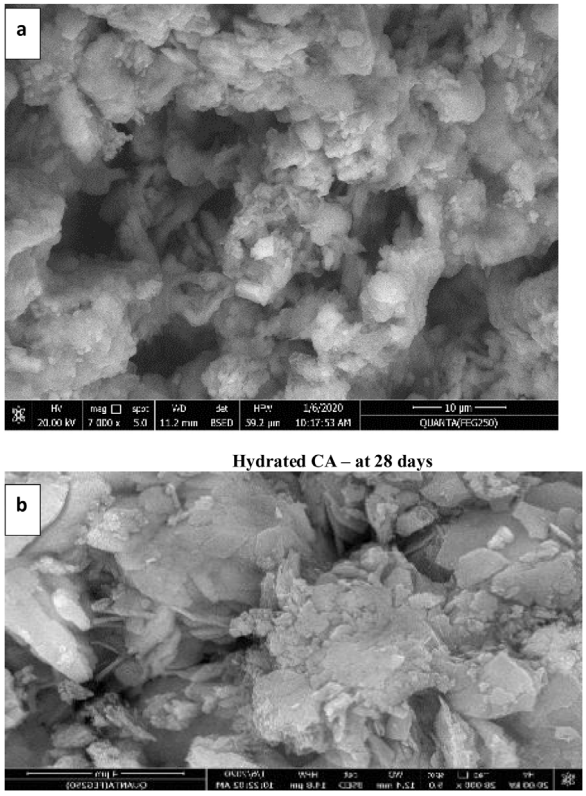

Fig. 11 – SEM images for calcined CA and C_3A at (1000 & 1200 °C) as in (a and b) respectively after hydration for 28 days.

mayenite as well as, a big size porous has been observed which causes a weak texture [7]. Fig. 11(b) illustrates the hydrated C_3A phase calcined at 1200 °C for 2 h cured in 100% humidity up to 28 days, which exhibits the presence of cubic C_3AH_6 and little amount of monoclinic AH_3 (gibbsite) due to the hydration of C_3A and conversion of metastable hydration products of small quantity of mayenite. Also, the texture is more compacted and homogenous as result of the presence a smaller size porous than in Fig. 11(a) of CA hydrated.

Table 1 represents the calculated values of compressive strength, bulk density as well as porosity percent of hydrated CA and C_3A at 28 days. The bulk density and the porosity percent values of CA are higher than C_3A hydrated phases. The hydration of CA is temperature dependent, at temperature less than 20 °C, CAH_{10} is produced. C_2AH_8 as well as AH_3 are produced at about 30 °C, Finally, C_3AH_6 and AH_3 are generated at temperature greater than 55 °C. Also, the conversion of CAH_{10} and C_2AH_8 to C_3AH_6 releases free water, which results in a decrease in strength due to higher porosity [28]. While in the case of C_3A only a small quantity of the hydration products from mayenite has been done. Also, C_3A has higher CaO/Al_2O_3 molar ratio which decreased the porosity and consequently increased the mechanical properties as discussed by [1]. The compressive strength value of CA is less than C_3A as a result of the conversion process of the hydration products and high difference in the porosity percent formed though the hydration of CA and C_3A phases. The physico-mechanical measurements are in good agreement with the SEM results.

The hydration of calcium aluminate phases are summarized as

$$CA + 10H \rightarrow CAH_{10} \quad (< 20\,^{\circ}C)$$

$$2CA + 11H \rightarrow C_2AH_8 + AH_3 \quad (\approx 30\,^{\circ}C)$$

$$3CA + 12H \rightarrow C_3AH_6 + AH_3 \quad (> 55\,^{\circ}C)$$

$$C_2AH_8 \rightarrow C_3AH_6 + 2AH_3 + 18H \quad [28]$$

Tricalcium aluminate phase (C_3A) hydrates very quickly known as 'flash-set' can occur on its own in water to form the hexagonal plate hydrates C_2AH_8 and C_4AH_{13} in the first instance which convert with time to the more stable cubic form C_3AH_6, or if the temperature is sufficiently high (>40 °C) directly to C_3AH_6 [29,30]. The chemical equation can be expressed as

$$2C_3A + 21H \rightarrow C_2AH_8 + C_4AH_{13} \rightarrow 2C_3AH_6 + 9H$$

Conclusion

Calcium aluminate phases such as CA as well as C_3A were successfully synthesized though sol–gel method. The nitrate salts of calcium and aluminum have been used as starting raw materials to prepare nano-oxides. The produced powder has been investigated by XRD, DLS, FTIR, SEM and TG/DTA techniques. The results concluded that increasing the CaO/Al_2O_3 molar ratio accelerate the formation of calcium aluminates phases at lower calcination temperature. Using Nano starting materials led to the formation of CA and C_3A at lower temperature than the traditional method, where CA has been formed at 1000 °C/1 h and C_3A was formed at 1200 °C/2 h. However it needs little higher temperature for obtaining high

pure phase percent. Dicalcium aluminate can't be obtained under the normal condition. The particles size of the product phases increased with increasing the calcination period (soaking time) as well as the calcination temperature, where it tends to coagulate. The bulk density and porosity of hydrated CA are higher than that of hydrated C_3A despite of the compressive strength of C_3A is higher than CA value.

REFERENCES

[1] M.F. Zawra, A.B. Shehata, E.A. Kishar, R.N. Yamani, Synthesis, hydration and sintering of calcium aluminate nanopowder for advanced applications, Comp. Rend. Chim. 14 (2011) 611–618.

[2] S. Yang, G. Xiao, D. Ding, Y. Ren, L. Lv, P. Yang, J. Gao, Solid-phase combustion synthesis of calcium aluminate with $CaAl_2O_4$ nanofiber structures, Ceram. Int. 44 (6) (2018) 6186–6191.

[3] A.B. Tchamba, J.C. Sofack, R. Yongue, U.C. Melo, Formulation of calcium dialuminate ($CaO{\cdot}2Al_2O_3$) refractory cement from local bauxite, J. Asian Ceram. Soc. 3 (2) (2015) 164–172.

[4] L.D. Mitchell, J.C. Margeson, J.J. Beaudoin, Synthesis and characterization of nanoparticulate calcium aluminates, in: Nanotechnology in Construction Conference, Paisley, Scotland, June 23, 2003, pp. 227–237.

[5] A.K. Chatterjee, G.I. Zhmoidin, Phase equilibrium diagram of the system calcium oxide-aluminum oxide-calcium fluoride, J. Mater. Sci. 7 (1972) 93–97.

[6] R.W. Nurse, J.H. Welch, A.J. Majumdar, The $CaO–Al_2O_3$ system in a moisture free atmosphere, Trans. Br. Ceram. Soc. 73 (1990) 15–23.

[7] H. Pollmann, Mineralogy and crystal chemistry of calcium aluminate cement, in: Calcium Aluminate Cements (CAC), International Conference on Calcium Aluminate Cements, 2001 in Book, Institute of Materials, vol. 757, 2001, pp. 79–119.

[8] V.K. Singh, M.M. Ali, U.K. Mandal, Formation kinetics of calcium aluminates, J. Am. Cerm. Soc. 73 (1990) 872–876.

[9] E.A. Levashov, A.S. Mukasyan, A.S. Rogachev, D.V. Shtansky, Self-propagating high-temperature synthesis of advanced materials and coatings, Int. Mater. Rev. 62 (4) (2017) 203–239.

[10] J.M. Rivas Mercury, A.H. De Aza, P. Pena, Synthesis of $CaAl_2O_4$ from powders: particle size effect, J. Eur. Ceram. Soc. 25 (2005) 3269–3279.

[11] G.H. Chen, Mechanical activation of calcium aluminate formation from $CaCO_3–Al_2O_3$ mixture, J. Alloy. Comp. 416 (2006) 279–283.

[12] S.W. Choi, S.H. Hong, Size and morphology control by planetary ball milling in $CaAl_2O_4:Eu^{2+}$ phosphors prepared by Pecini method and their luminescence properties, Mater. Sci. Eng. B 171 (1–3) (2010) 69–72.

[13] R.E. Moore, R. Hong-Sang, Chemical synthesis of monocalcium aluminate powders, Bol. Soc. Esp. Ceram. Vidr. 32 (6) (1993) 369–376.

[14] P.S. Behera, R. Sakar, S. Bhattacharyya, Nanoalumina: a review of the powder synthesis method, Interceram-Int. Ceram. Rev. 65 (1–2) (2016) 10–16.

[15] M.A. Alavi, A. Morsali, Ultrasonic-assisted synthesis of $Ca(OH)_2$ and CaO nanostructures, J. Exp. Nanosci. 5 (2) (2010) 93–105.

[16] A. Roy, J. Bhattacharya, Synthesis of $Ca(OH)_2$ nanoparticles by wet chemical method, Micro Nano Lett. 5 (2) (2010) 131–134.

[17] Z. Tang, D. Claveau, R. Corcuff, K. Belkacemi, J. Arul, Preparation of nano-CaO using thermal-decomposition method, Mater. Lett. 62 (14) (2008) 2096–2098.

[18] B.K. Olega, L. Isabelle, V. Alexander, K.J. Kenneth, Alkaline-earth oxide nanoparticles obtained by aerogel methods. Characterization and rational for unexpectedly high surface chemical reactivities, Chem. Mater. 9 (11) (1997) 2468–2480.

[19] Ö. Kirca, Temperature Effect on Calcium Aluminate Cement Based Composite Binders, Ph.D. thesis in Civil Engineering, Middle East Technical University, Turkey, 2006.

[20] E. De La Rosa, Designation: C191-08 Standard Test Methods for Time of Setting of Hydraulic Cement by Vicat Needle, ASTM Standard, 2009.

[21] H. El-Didamony, A.A. Amer, H. Abd Ela-ziz, Properties and durability of alkali-activated slag pastes immersed in sea water, Ceram. Int. 38 (2012) 3773–3780.

[22] A. Adams, P.A. Romans, Analytical methods for determining from thermal decoposition of aluminum nitrate nonahydrate Report of Investigations, vol. 9146, United States Bureau of Mines, 1987.

[23] C. Ettarh, A.K. Galwey, A Kinetic and mechanistic study of the thermal decomposition of calcium nitrate, Thermochim. Act. 288 (1996) 203–219.

[24] J. Paulik, F. Paulik, M. Arnold, Thermogravimetric examination of the dehydration of calcium nitrate tetrahydrate under quasi-isothermal and quasi-isobaric condition, J. Therm. Anal. 27 (2) (1983) 409–418.

[25] P.K. Kiyohara, H.S. Santos, A.C.V. Coelho, P.D.S. Santos, Structure, surface area and morphology of aluminas from thermal decomposition of $Al(OH)(CH_3COO)_2$ crystal, Ana. Acad. Bras. Cien. 72 (2000) 471–495.

[26] P.S. Aggarwal, J.A. Gard, F.P. Glasser, G.M. Biggar, Synthesis and properties of dicalcium aluminate, Cem. Concr. Res. 2 (1972) 291–297.

[27] F.I. Azo, Y.X. Yang, D. Panias, L. Kolbeinsen, J. Safarian, Leaching characteristics and mechanism of the synthetic calcium-aluminate slags for alumina recovery, Hydrometallurgy 185 (2019) 273–290.

[28] J.F. Zapata, M. Comez, H.A. Colorado, Characterization of two calcium aluminate cement pastes. Ch. 45: Advances in high temperature ceramic matrix composites and materials for sustainable development, Ceram. Trans. 263 (2017) 491–503.

[29] S.N. Ghosh, Advances in cement technology, in: Critical Reviews and Case Studies on Manufacturing, Quality Control, Optimization and Use, 1st edn, Pergamon Press Ltd, 1983, pp. 311.

[30] H.F.W. Taylor, Cement Chemistry, 1st edn, Academic Press, 1990.